Environmental Earth Sciences (2023) 82:219
https://doi.org/10.1007/s12665-023-10915-1

ORIGINAL ARTICLE

Characterization of groundwater aquifers using hydrogeophysical and hydrogeochemical methods in the eastern Nile River area, Khartoum State, Sudan

Musaab A. A. Mohammed[1,2] · Norbert P. Szabó[1,3] · Péter Szűcs[1,3]

Received: 14 October 2022 / Accepted: 9 April 2023 / Published online: 25 April 2023

Abstract
The primary goals of this research are to detect the spatial variation of the hydrogeological characteristics and evaluate the groundwater quality in the eastern Nile River, Khartoum state, Sudan, using geophysical and hydrochemical methods. Thirteen Vertical electrical soundings (VES), using Schlumberger configuration, were measured along three profiles to characterize the groundwater aquifer. VES findings denoted that the study area comprises two hydraulically connected aquifers. The upper aquifer of sand has an average thickness of 50 m, and the lower aquifer is composed of sandstone of a thickness of up to 300 m. The results of VES inversion were further used to measure aquifer characteristics, including transverse resistance, longitudinal conductance, hydraulic conductivity, and transmissivity. The detected average values of these parameters were 6690 Ωm^2, 1.4 Ω^{-1}, 264 m^2/d and 4 m/day, respectively. In addition, regression analysis was performed to suggest local relationships for estimating aquifer characteristics within the study area. On the other hand, total longitudinal conductance was used to predict the protective strength of the hydrogeological columns, ranging from 1.7 to 5.8 Ω^{-1}; as a result, the protective capacity of the aquifer ranged from good to very good, suggesting potable water quality. This result was subsequently confirmed by the groundwater quality index (GWQI) model. Eleven physiochemical parameters analyzed for nine boreholes were used in GWQI estimation to assess groundwater quality in the study area. The primary analysis of the hydrochemical parameters indicated that almost all parameters are below permissible limits prescribed by the World Health Organization (WHO). The computed GWQI varies between 34.8 and 148, and the majority of groundwater samples, precisely 55.5%, are good water types, while 22.2% of the samples are in an excellent quality state. This research concluded that the groundwater aquifer in the study area is ideal for groundwater exploitation. However, applying a detailed geophysical and hydrochemical survey is recommended to reduce the uncertainty of the resulting models.

Keywords Khartoum · Nile River · Nubian aquifer · Dar Zarrouk · Hydrogeological parameter · Groundwater quality

Introduction

Groundwater is the primary source of water supply in arid and semi-arid areas, especially when there are no surface water resources (Mohammed 2020). The Eastern Nile River area is densely populated agricultural land with few water resources used mainly for drinking and irrigation purposes (Mohammed et al. 2022c). In recent decades, one of the major priorities of local and national governments has been to regulate and limit groundwater usage for agricultural purposes to preserve and protect this valuable resource. Nevertheless, agriculture plays an important role in socioeconomic development. Therefore, groundwater resources had to be evaluated to achieve sufficiency for human consumption and agriculture. Comprehensive research, including hydrogeological, hydrogeochemical and geophysical studies, must be carried out to for delineation and characterization of groundwater resources to fulfil water supply sustainability.

The geometry and the hydrogeological parameters are the basis for evaluating groundwater resources.

✉ Musaab A. A. Mohammed
musab20501@gmail.com

1 Faculty of Earth Science and Engineering, University of Miskolc, Miskolc 3515, Hungary

2 College of Petroleum Geology and Minerals, University of Bahri, Khartoum, Sudan

3 MTA-ME Geoengineering Research Group, University of Miskolc, Egyetemváros, Hungary

Transmissivity and hydraulic conductivity as crucial hydrogeological parameters are essential in assessing the aquifer's productivity (Szabó 2015). These parameters describe the rate at which water moves in the porous media and thus give information about aquifer yield and groundwater reserves (Mohammed et al. 2023b). Pumping tests are the most widely employed to detect the hydraulic parameters of groundwater aquifers. However, these tests are costly and time-consuming, and detecting the spatial distribution of the measured parameters is difficult in heterogenous aquifer systems. On the other hand, groundwater quality assessment is crucial, since it determines its suitability for different purposes. Groundwater quality is influenced by natural and artificial activities which allow dissolution, precipitation, and infiltration of physical and chemical pollutants into the groundwater, changing the composition of groundwater. The assessment and monitoring of groundwater quality are crucial concerns that have a major impact on human health. Around 80% of all human diseases are water-borne, according to the World Health Organization (Edition 2011). Therefore, the comprehensive assessment of groundwater aquifers regarding quantity and quality is crucial for successful water resource management.

Electrical resistivity as a non-invasive method is widely employed in hydrogeological investigations. This method was successfully applied to detect the thickness of the aquifer, depth to the water table and hydraulic parameters in less time and cost-effectively. Vertical electrical sounding (VES) is the most widely applied resistivity technique in the delineation of groundwater potential zones and determination of the hydraulic parameters (Gugulothu et al. 2020; Araffa et al. 2021; Oyeyemi et al. 2021; Stanly et al. 2021; Daud et al. 2022; Ige et al. 2022; Muhammad et al. 2022; Nugraha et al. 2022). Recent developments in computer-based software have guided researchers to link the product of VES inversion and hydraulic parameters. Maillet (1947) first introduced Dar Zarrouk parameters to measure the longitudinal conductance and transverse resistance of the geoelectrical layers. Niwas and Singhal (1981) have successfully developed an analytical relationship between Dar Zarrouk parameters and aquifer transmissivity by employing the analogy between Darcy's law of groundwater flow and Ohm's law of electric movement. Studies about using Dar Zarrouk parameters in aquifer characterization are widely reported in the literature (Attwa et al. 2014; Akhter and Hasan 2016; de Almeida et al. 2021; Eyankware et al. 2022; Mahmud et al. 2022). In addition, Dar Zarrouk criteria have been employed to assess the aquifers' susceptibility to surface and subsurface contamination. The detection of vulnerable areas and the creation of remediation plans are aided by the evaluation of the groundwater aquifer's protective capacity (Oladapo and Akintorinwa 2007). These developed connections made the electrical resistivity method a fundamental technique for groundwater investigations.

In the eastern Nile River area, rigorous groundwater quality assessment is required as the foundation for strategy implementation, since groundwater is mainly used for human consumption. The conventional methods for evaluating and monitoring groundwater quality rely on comparing analyzed physiochemical parameters to national or global standards. Assessment of groundwater quality using these traditional techniques is costly and time-consuming. To overcome these limitations, many experts have developed several water quality indices (WQIs) to assess surface and groundwater suitability for drinking and irrigation purposes (Brown et al. 1970; Boateng et al. 2016; Sharifinia et al. 2017; Asadi et al. 2020; Kanga et al. 2020; Zhang et al. 2022). WQI is a detailed index that combines physical, chemical, and biological parameters of water quality to produce an index that decision and policymakers can quickly grasp. In this research, the weighted arithmetic groundwater quality index (GWQI) is developed to assess groundwater quality in the eastern Nile River area.

The recent research attempts to comprehensively characterize groundwater aquifers in the eastern Nile River area in northern Khartoum state, Sudan. The main aim of this study is to integrate geophysical and hydrogeochemical methods to delineate potential groundwater zones, detect the spatial distribution of the hydrogeological parameters, and evaluate groundwater quality and its suitability for domestic uses. The outcomes of this research will improve groundwater management scenarios and thus lead to water supply sustainability.

Study area

The study area is located in the eastern Nile River in north Khartoum state, Sudan, and covers about 598 km^2 bounded by decimal longitude from 32° 30′ to 32° 43′ and latitude from 15° 36′ to 1° 51′ (Fig. 1). Since central Sudan is situated in the Savanna belt, the average annual precipitation ranges from 100 to 200 mm/year. The eastern Nile River area features a flat peneplain topography. These plains progressively ascend from 350 m in the west part of the region to 500 m above mean sea level (m.s.l) in the east. Around 80% of the population in the study region resides near the Nile River, and population density gradually decreases farther from the Nile. The 2008 census showed 9 million people living in Khartoum, a significant rise in population over the previous 50 years. The research area is part of the Khartoum sub-basin and is located on the northern periphery of the Nile rift basin. The Pan-African Basement Complex confines this continental sub-basin to the northeast and southwest and defines its bottom limit at a depth of more than 500 m (Köhnke et al. 2017). The geological

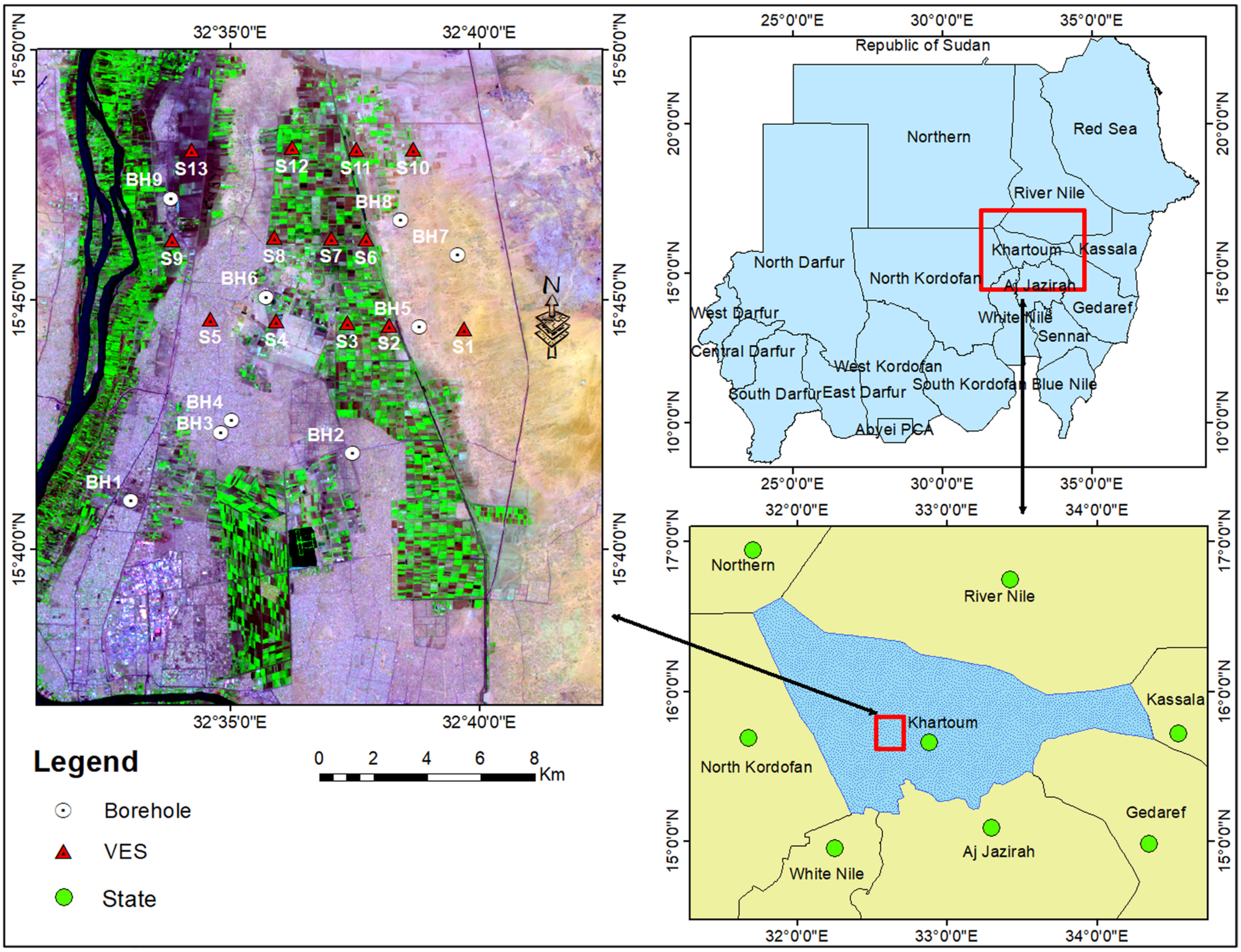

Fig. 1 Geographical map showing the location of the study area in Khartoum state

succession comprises three rock types: Precambrian basement rocks, Cretaceous Nubian formation, and recent deposits. Gneisses, schists, and granites constitute the basement rocks, and their depths range from zero when exposed at the surface, mostly on the north and east borders of the region, to up to 500 m in the south (Hussein and Awad 2006). Underlying the Precambrian basement rocks is the Cretaceous Nubian formation, which mainly consists of mudstone and sandstone (Kheiralla 1966). The main groundwater aquifer in the Khartoum basin is the Nubian formation. Recent deposits in the study region include alluvium wadi deposits and windblown deposits in depths ranging from 3 to 15 m (Haggaz and Kheirallah 1988). Figure 2 shows the geological map of the study area in which the main rock units and geological structure are presented. Groundwater is found in the weakly cemented Nubian formation in the Khartoum basin under confined to semiconfined conditions due to the presence of thin to thick aquitards (Abdelsalam et al. 2016). In the research area, two main groups of the recharged groundwater can be identified: Nilotic and Meteoric water (Farah et al. 2000). Nilotic groundwater infiltrated from the Niles and retained in upper and lower aquifers within a 12 km radius of the Nile River. Meteoric groundwater recharged in the regions outside the Nile influence. Groundwater levels in the study area range from 341 m in the western part to 356 m in the eastern part. The higher water level in the western parts is mainly due to the extensive recharge from the Nile River. As a result, the main groundwater flow direction in the Nubian aquifer is from the west to the central and eastern parts of the study area (Fig. 3).

Methodology

Electrical resistivity survey

This study employed vertical electrical sounding (VES) techniques to characterize groundwater aquifers in the eastern Nile River area in northern Khartoum state. Thirteen

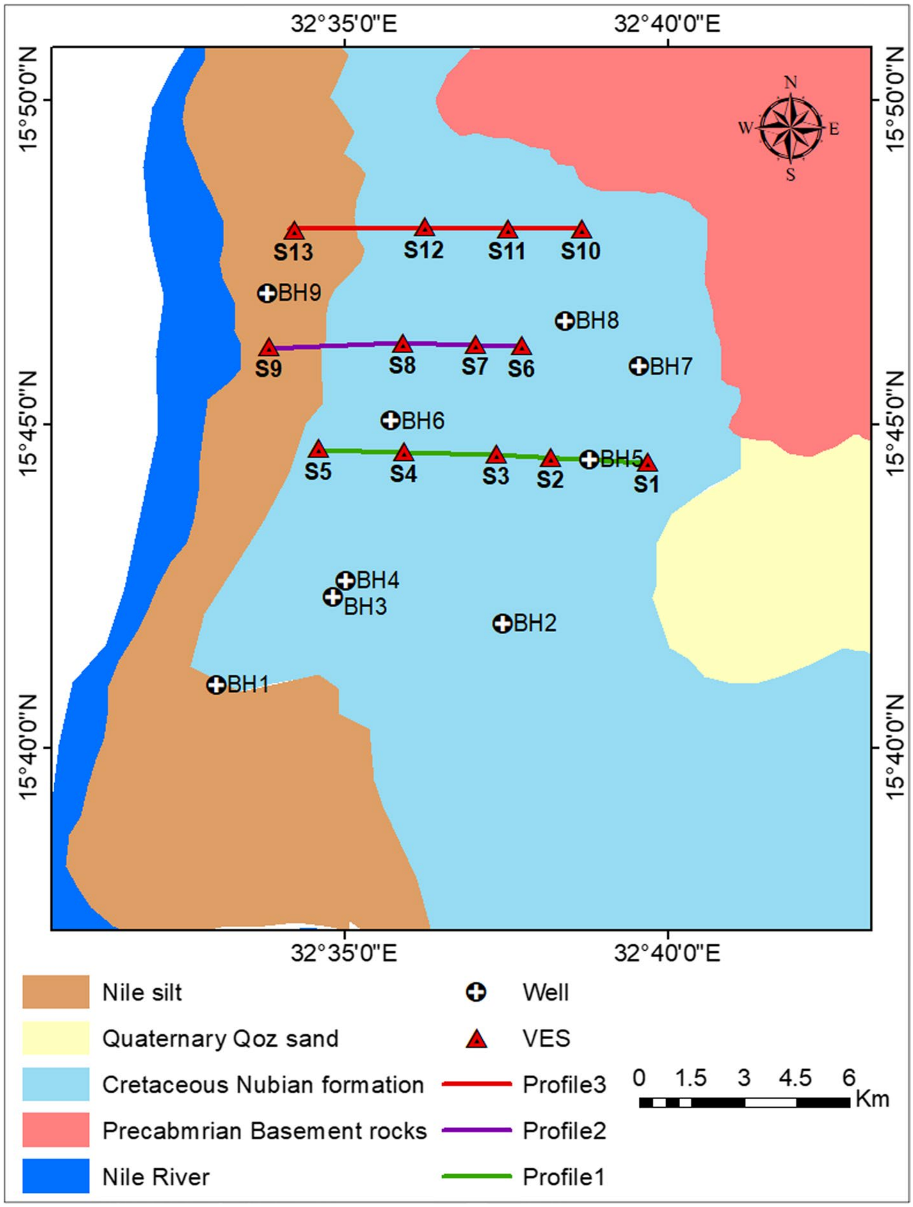

Fig. 2 Geological map of the study area modified after (Hussein and Awad 2006)

VES points were measured using Schlumberger configuration with electrode spacing (AB/2) of 900 m. The data were acquired using ABEM SAS 100 resistivity meter, and the VES points were measured along three profiles. The fundamental drawback of the geophysical inversion is the nonuniqueness of the derived solution, which results in a murky interpretation of the model. To solve this problem, a priori data on the geological phenomena must be gathered to provide a credible interpretation. This study used lithological logs obtained from eight boreholes to validate the resulting geoelectrical models.

Dar Zarrouk parameters were used to measure the aquifer characteristics, including transverse resistance (R) (Ωm^2), longitudinal conductance (S) (Ω^{-1}) and transmissivity (T) (m^2/d). The inspiration behind using Dar Zarrouk parameters for hydrogeological parameters detection is that groundwater flow is influenced by the same petrophysical factors that influence current flow, such as porosity, water saturation, and permeability (Niwas and Singhal 1981). Figure 4 describes Dar Zarrouk parameters as an analogy between groundwater and electrical current flow. The hydraulic conductivity (K) (m/d) is measured empirically using a formula suggested by (Heigold et al. 1979) based on the connection between the electrical resistivity of the porous aquifer and hydraulic conductivity. These parameters are calculated using Eqs. 1–5 as

$$S = \frac{h}{\rho} = \sum_{i=1}^{n} \frac{h_i}{\rho_i} \tag{1}$$

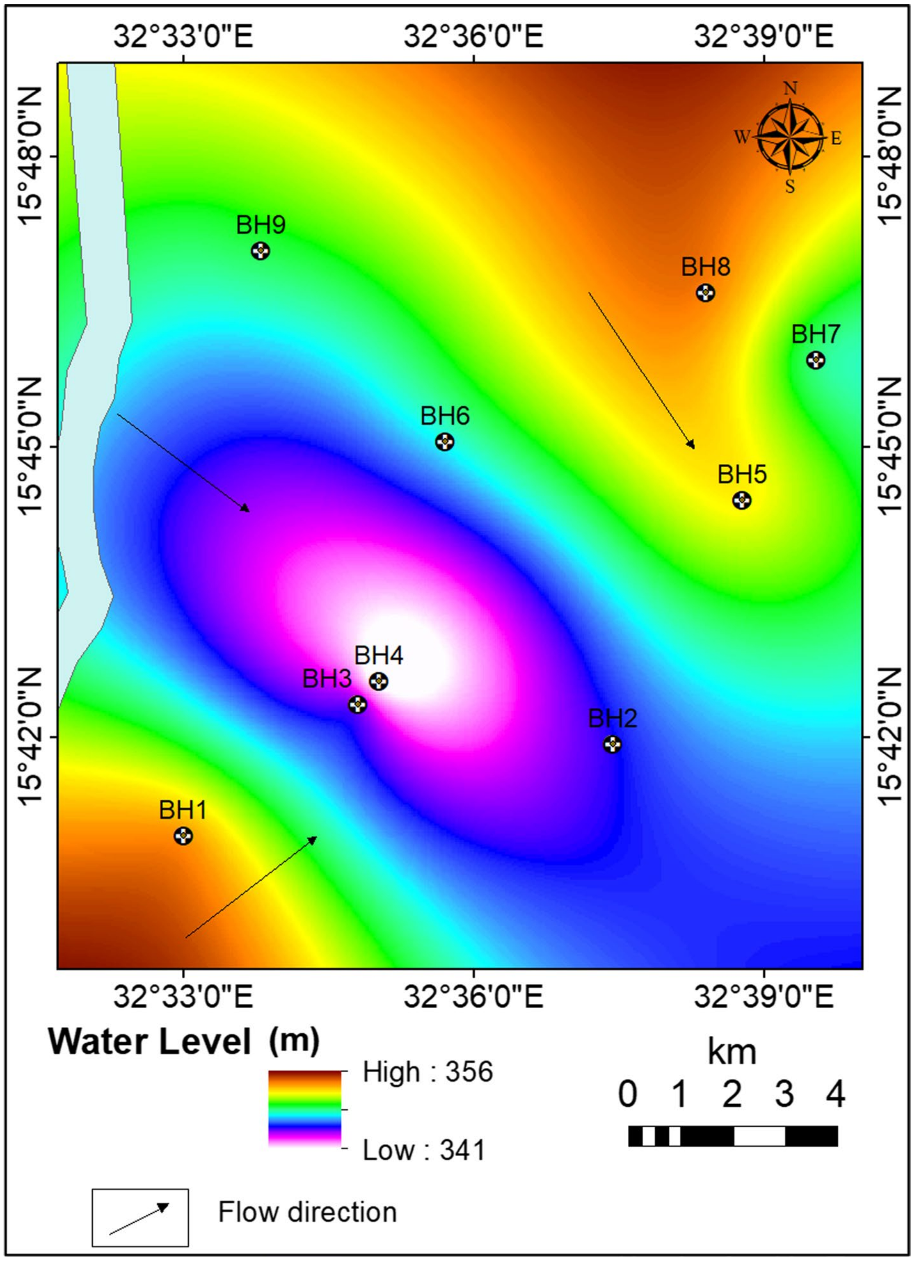

Fig. 3 Water level map showing the main flow direction of groundwater

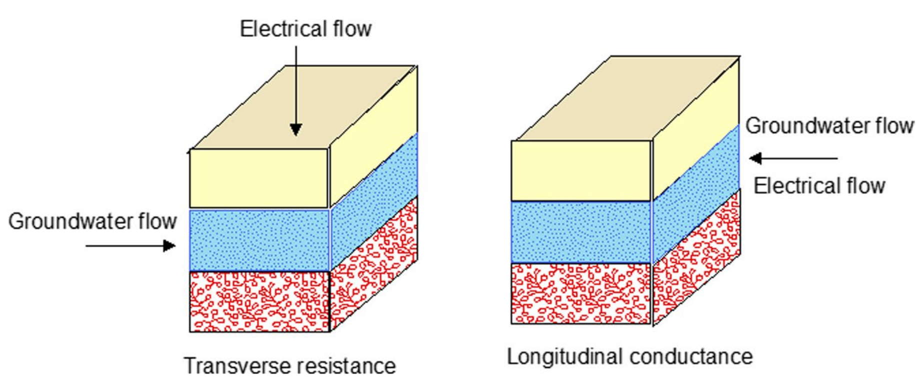

Fig. 4 Dar Zarrouk parameters on a unit cross-sectional layered model modified after (Kelly and Reiter 1984)

Table 1 Protective capacity classes based on Oladapo and Akintorinwa (2007)

Protective capacity class	Total longitudinal conductance (mho)
Poor	< 0.1
Weak	0.1–0.19
Moderate	0.2–0.69
Good	0.7–4.9
Very good	5–10
Excellent	> 10

$$R = h * \rho = \sum_{i=1}^{n} h_i * \rho_i \quad (2)$$

$$T = \mathrm{K\sigma R} \quad (3)$$

$$T = \frac{\mathrm{KS}}{\sigma} \quad (4)$$

$$K = 386.4R_{\mathrm{aq}}^{-0.93283} \quad (5)$$

where σ and K represent electrical and hydraulic conductivity, respectively, while n, ρ, and h represent layers number, resistivity and thickness of the layers, respectively. R_{aq} represents the resistivity of the aquifer layer.

In this research, the longitudinal conductance was further used to predict the protective capacity of the groundwater aquifers using a categorization proposed by (Oladapo and Akintorinwa 2007). The vulnerability of aquifers to subsurface and surface contamination is revealed by the capacity of the geological column to retain the pollution. High layer thickness and, thus, the highest protection for the aquifer are associated with the highest longitudinal conductance and vice versa. The classification of the geological column based on the longitudinal conductance is illustrated in Table 1.

Pumping tests analysis

In this study, Cooper Jr and Jacob (1946) method is applied to measure the transmissivity and hydraulic conductivity from boreholes installed in different aquifer zones. This method involves fitting a straight line in a semi-logarithmic scale of a plot between time and drawdown (s) to determine the average drawdown (Δs) and transmissivity. In this research, the test duration lasted from 150 to 200 min until the steady-state condition was fulfilled. The detected hydrogeological parameters from the Dar Zarrouk approach are compared to the pumping test result to ensure a reliable interpretation and conceptualization of the hydrogeological system. The transmissivity and hydraulic conductivity

Table 2 Assignment of weights and the relative weights to the studied groundwater quality parameters

Parameters/units	Weight (wi)	Relative weight (Wi)
pH	2	0.05
EC µS/cm	3	0.08
TDS mg/L	5	0.13
TH mg/L	4	0.10
Ca^{2+} mg/L	4	0.10
Mg^{2+} mg/L	4	0.10
Na^{+} mg/L	4	0.10
Cl^{-} mg/L	4	0.10
SO_4 mg/L	4	0.10
HCO_3 mg/L	3	0.08
NO_3 mg/L	3	0.08

Table 3 Classification of groundwater based on GWQI as given by Ramakrishniah et al. (2009)

WQI range	Class	Type of water
< 50	I	Excellent water
50.1–100	II	Good water
100.1–200	III	Poor water
200.1–300	IV	Very poor water
> 300	V	Unsuitable water

using Cooper Jr and Jacob (1946) method are measured using Eqs. 6 and 7 as

$$\Delta s = \frac{2.3Q}{4\pi T} \quad (6)$$

$$T = K * b \quad (7)$$

where Q is the pumping rate, and b is the thickness of the aquifer.

Hydrogeochemical analysis

The hydrogeochemical analysis is performed using routinely analyzed physiochemical parameters to assess the groundwater chemistry in the study area. The investigation was achieved by comparing the detected parameters with a given standard, revealing the hydrochemical facies and calculating the groundwater quality index (GWQI).

To assess the quality of the groundwater in the eastern River Nile region of northern Khartoum State, Sudan, nine groundwater samples were collected during the post-monsoon season of 2018. The boreholes used for the groundwater sampling were installed privately and ranged in depth

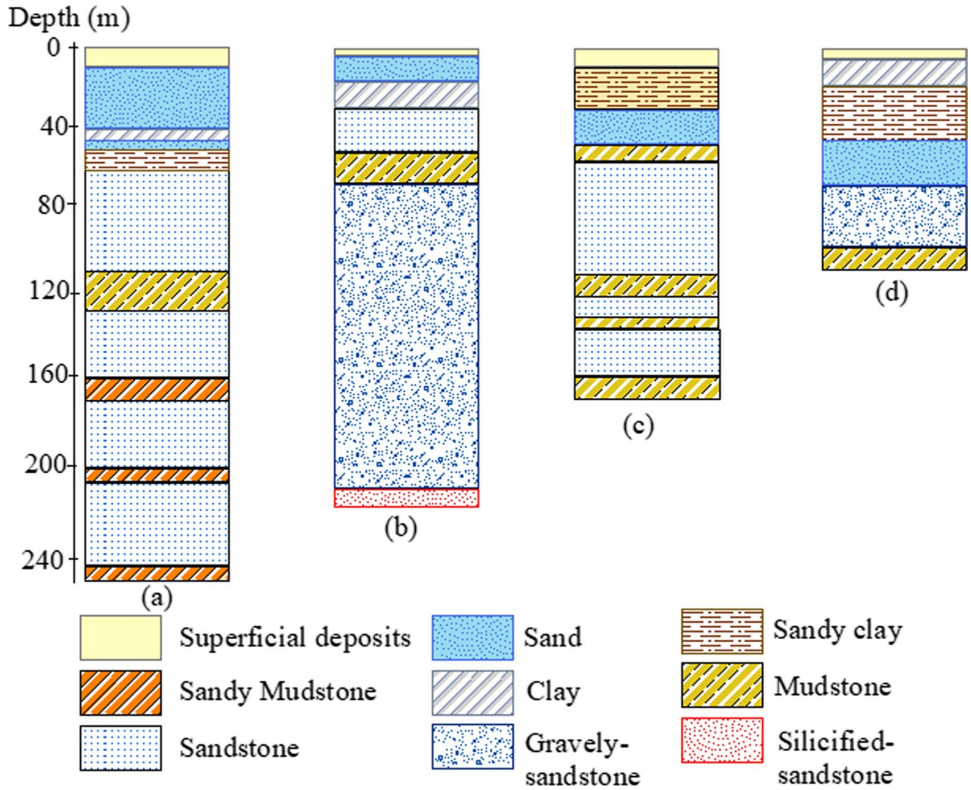

Fig. 5 Example of the lithological logs of the boreholes used in the interpretation of the VES data

from 100 to 260 m. The geographical distribution of the samples is shown in Fig. 1. Groundwater samples were analyzed for physicochemical parameters in Khartoum State Water Corporation (KSWC) labs. These parameters are total hardness (TH), calcium (Ca^{+2}), sodium (Na^{+}), magnesium (Mg^{+2}), chloride (Cl^{-}), nitrate (NO_3^{-}), sulfate (SO_4^{-2}), bicarbonate (HCO_3^{-}), Electrical conductivity (EC), total dissolved solids (TDS), and hydrogen ion activity (pH). The accuracy of the hydrochemical analysis was tested by a formula (Eq. 8) suggested by (Appelo and Postma 2005) to calculate the electrical balance (EB) between the cations and anions expressed in milliequivalents per liter (meq/L). In this research, EB% is ranged within ± 10%.

$$(EB\%) = \frac{\sum \text{cations} - \sum \text{anions}}{\sum \text{cations} + \sum \text{anions}} \times 100 \tag{8}$$

GWQI model is considered a dimensionality reduction technique that simplifies the analyzed chemical, physical and biological parameters of groundwater quality into a single water quality index (Mohammed et al. 2022a). GWQI models are developed in three steps, which include assigning weights, computing the rating scale, and aggregating sub-indices. In this study, the weights were assigned based on the author's knowledge and available literature to reveal the influence rate for each physiochemical parameter in groundwater quality. The most crucial variable is assigned a weight of 5, while the least relevant variable is assigned a weight of 2. As a result, Eq. 9 is used to determine the relative weight (Wi) for the parameters (Singh 1992). The result of the assigned and relative weight is shown in Table 2. In the second stage, the rating scale is calculated (Eq. 10). The purpose of scaling is to convert all the chosen physiochemical parameters into a single scale, considering the physiochemical parameters generally have distinct units and ranges. The rating scale was acquired using the standard limits prescribed by WHO (Edition 2011). The sub-indices with their weights are aggregated in the last step in the WQI computation. In this study, the final index value was calculated using Eqs. 11 and 12 after the sub-index aggregation was completed using the mean arithmetic technique (Tiwari and Mishra 1985). Consequently, groundwater samples are classified according to their GWQI into five classes (Table 3), as suggested by (Ramakrishniah et al. 2009)

$$\text{Wi} = \frac{\text{wi}}{\sum_{i=1}^{n} \text{wi}} \tag{9}$$

$$\text{Ri} = \frac{\text{Xi}}{\text{Xs}} * 100 \tag{10}$$

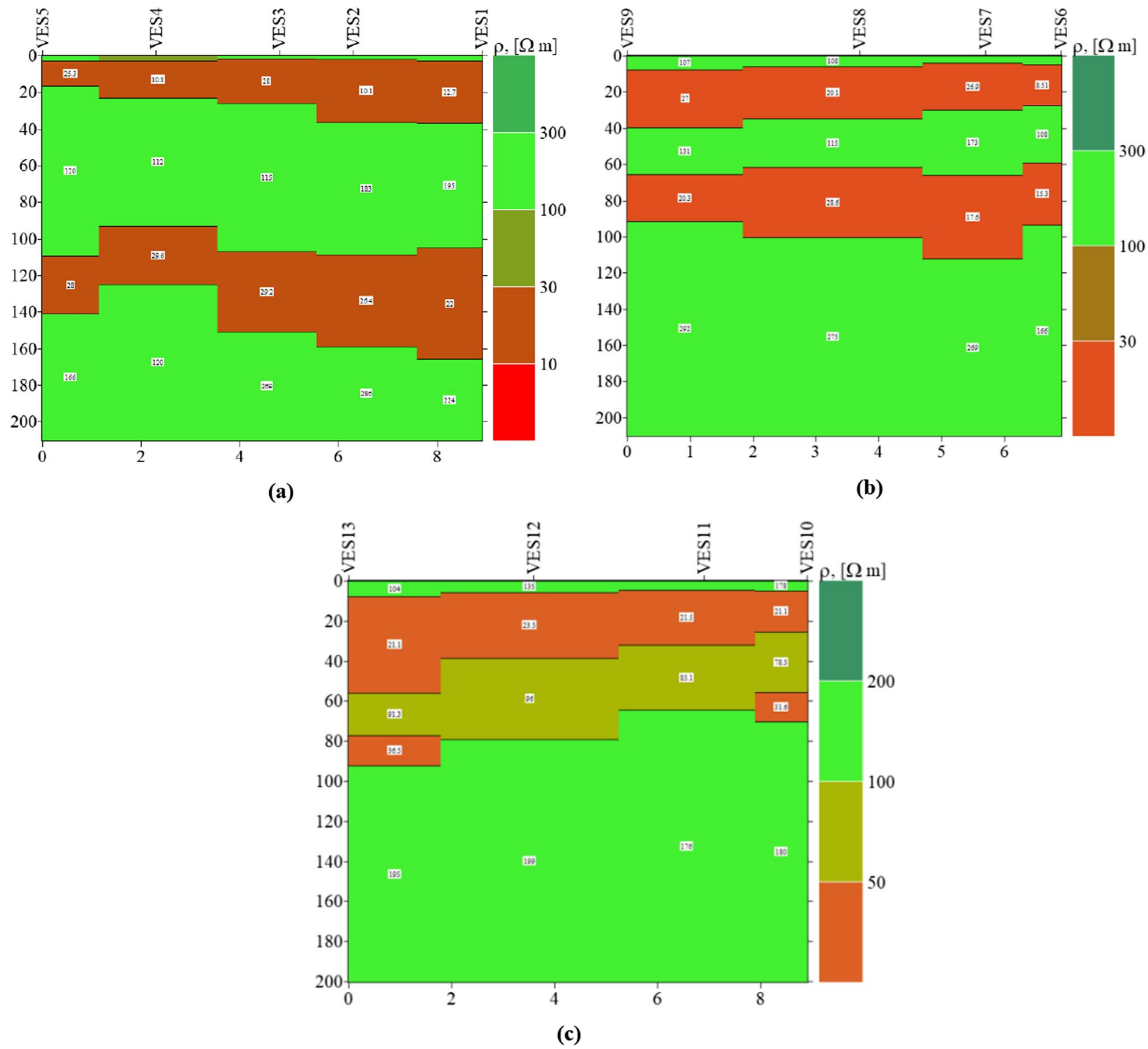

Fig. 6 Resistivity cross sections of **a** profile 1, **b** profile 2, and **c** profile 3

$$SI = Wi * Ri \quad (11)$$

$$WQI = \sum SI \quad (12)$$

Wi and wi represent the relative weight and assigned weight allocated to the parameters. Ri is the rating scale value, while Xi and Xs are the actual and standard values for the parameters, respectively. SI is the sub-index for n number of physiochemical parameters.

Results and discussion

Delineation of groundwater aquifers

Vertical electrical sounding (VES) is used to delineate the potential zones for groundwater using the true resistivities and layer thickness resulting from the 1D inversion of the field curves. The least number of layers considered essential and quantitatively detectable on the field curve were used to

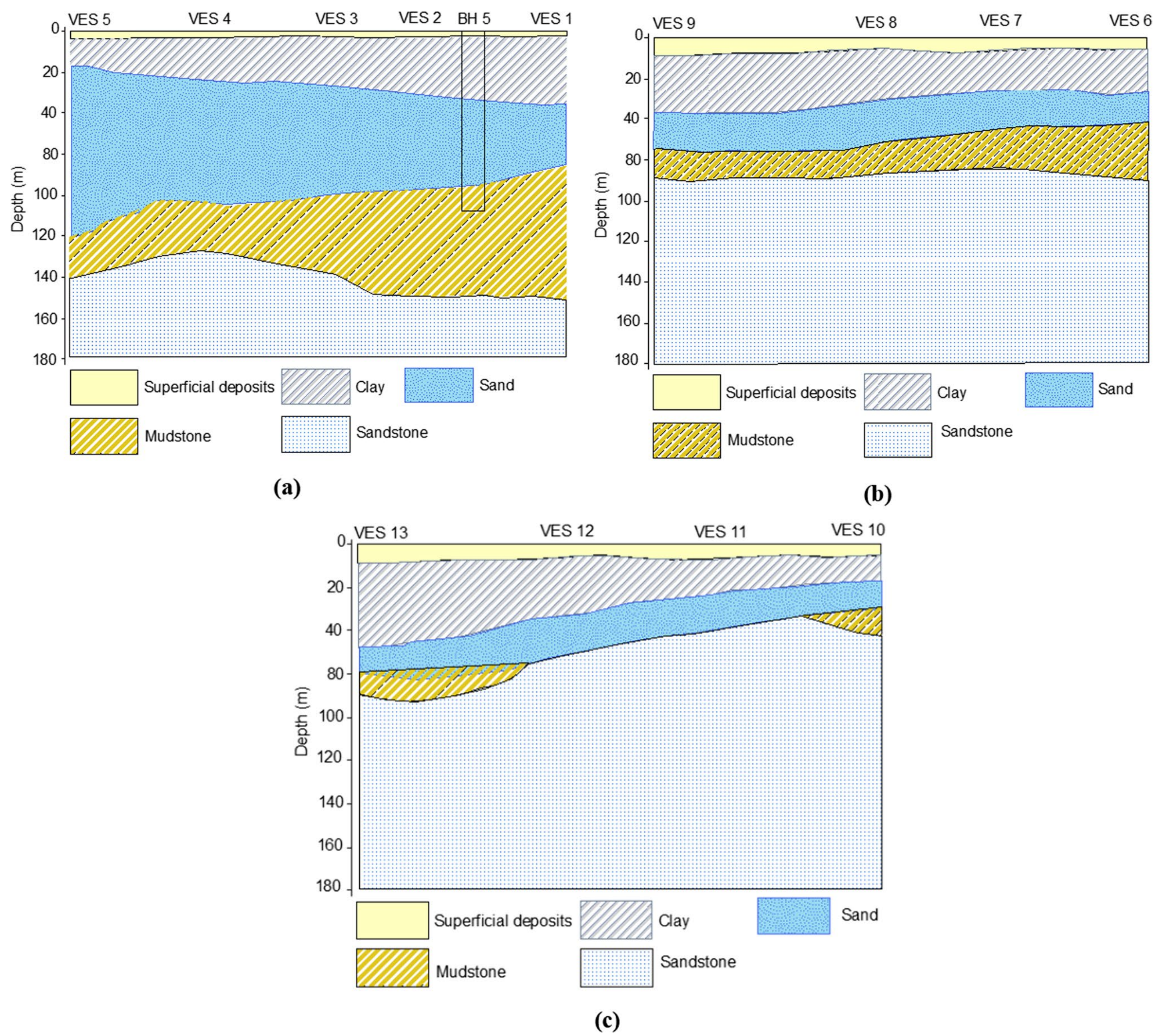

Fig. 7 Hydrogeological cross sections of **a** profile 1, **b** profile 2, and **c** profile 3

interpret the VES data. Other layers may not be immediately apparent; these hidden layers are suppressed in this case. Only include concealed layers if nearby borehole logs indicate their presence or create a satisfactory fit. Lithological logs obtained from 8 boreholes (Fig. 5a, b, c, and d) are used to help interpret VES curves. In this research, three resistivity cross sections extending E–W are settled (Fig. 6). Based on the correlation between VES curves and lithological logs, the resistivity cross sections are converted to hydrogeological cross sections (Fig. 7) to reveal the thicknesses of the aquifers and aquitards and map the geological structures that may influence the presence and movement of groundwater.

Profile 1 comprises 5 VES points (S 1, S 2, S 3, S 4, and S 5), and the lithological log of BH 5 guides the interpretation. This profile consists of 5 geological units (Figs. 6a and 7a). Superficial deposits with resistivity range from 52 to 243 Ωm and an average thickness of 1.8 m, followed by a clay layer with average thickness and resistivity of 23 m and 17 Ωm, respectively. The third layer is saturated sand with an average thickness of 50 m. The thickness of the aquifer changes gradually from 20 m in VES 1 in the eastern part to more than 80 m in VES 5. The fourth layer is a mudstone layer with a thickness range from 20.4 to 60.7 m and resistivity between 22 and 29.6 Ωm. This previous layer serves as an aquitard which separates the upper aquifer from the lower. The lower aquifer is a thick, saturated layer of coarse sandstone with an average resistivity of 200 Ωm.

Table 4 Measured Dar Zarrouk parameters and their correspondence hydrogeological parameters for the detected aquifers in the study area

VES no	Layer	ρ (Ωm)	h (m)	R (Ωm^2)	S (Ω^{-1})	Layer lithological description	K (m/d)	T (m^2/d)	Σ S (Ω^{-1})
1	1	158	2.89	456.6	0.02	Superficial deposits	–	–	5.8
	2	12.7	34.3	435.6	2.7	Clay	–	–	
	3	195	67.9	13,240.5	0.35	Sand (Aquifer)	2.82	191.7	
	4	22	60.7	1335.4	2.76	Mudstone	–	–	
	5	224	–	–	–	Sandstone (aquifer)	2.48	–	
2	1	123	1.87	230	0.02	Superficial deposits	–	–	5.8
	2	10.1	34.8	351.5	3.45	Clay	–	–	
	3	183	72	13,176	0.39	Sand (Aquifer)	2.99	215.7	
	4	26.4	50.4	1330.6	1.9	Mudstone	–	–	
	5	286	–	–	–	Sandstone (aquifer)	1.97	–	
3	1	220	1.81	398.2	0.008	Superficial deposits	–	–	3
	2	28	24	672	0.86	Clay	–	–	
	3	115	81.1	9326.5	0.7	Sand (Aquifer)	4.62	374.7	
	4	29.3	43.7	1280.4	1.5	Mudstone	–	–	
	5	269	–	–	–	Sandstone (aquifer)	2.09	–	
4	1	52.4	2.69	141	0.05	Superficial deposits	–	–	3.6
	2	10.8	20.4	220.3	1.9	Clay	–	–	
	3	112	70.2	7862.4	0.63	Sand (Aquifer)	4.73	332.5	
	4	29.6	31.7	938.3	1.07	Mudstone	–	–	
	5	120	–	–	–	Sandstone (aquifer)	4.44		
5	1	243	2.92	709.6	0.01	Superficial deposits	–	–	2.4
	2	25.3	13.7	346.6	0.54	Clay	–	–	
	3	120	93	11,160	0.78	Sand (Aquifer)	4.44	413	
	4	28	20.4	879.2	1.12	Mudstone	–	–	
	5	166	–	–	–	Sandstone (aquifer)	3.28	–	
6	1	104	4.93	512.7	0.05	Superficial deposits	–	–	5.3
	2	8.51	22.7	193.2	2.7	Clay	–	1-	
	3	108	31.5	3402	0.29	Sand (Aquifer)	4.9	154.3	
	4	15.3	34.5	527.8	2.25	Mudstone	–	–	
	5	166	–	–	–	Sandstone (aquifer)	3.28	–	
7	1	217	4.19	909.2	0.02	Superficial deposits	–	–	3.8
	2	26.9	25.6	688.6	0.95	Clay	–	–	
	3	173	36.2	6262.6	0.21	Sand (Aquifer)	3.15	114.2	
	4	17.6	46.2	813.1	2.62	Mudstone	–	–	
	5	269	–	–	–	Sandstone (aquifer)	2.09	–	
8	1	108	5.91	638.2	0.05	Superficial deposits	–	–	3
	2	20.1	29.1	584.9	1.45	Clay	–	–	
	3	115	26.4	3036	0.23	Sand (Aquifer)	4.62	122	
	4	28.6	39.1	1118.2	1.37	Mudstone	–	–	
	5	275	–	–	–	Sandstone (aquifer)	2.04	–	
9	1	107	7.5	802.5	0.07	Superficial deposits	–	–	2.7
	2	27	32.1	866.7	1.19	Clay	–	–	
	3	131	25.9	3392.9	0.19	Sand (Aquifer)	4.09	105	
	4	20.3	25.9	525.8	1.27	Mudstone	–	–	
	5	292	–	–	–	Sandstone (aquifer)	1.93	–	
10	1	104	7.6	790.4	0.07	Superficial deposits	–	–	3
	2	21.1	48.3	1019.1	2.28	Clay	–	–	
	3	91.3	21.4	1953.8	0.23	Sand (Aquifer)	5.73	122.6	
	4	36.5	15.2	554.8	0.42	Mudstone	–	–	
	5	195	–	–	–	Sandstone (aquifer)	2.82	–	

Table 4 (continued)

VES no	Layer	ρ (Ωm)	h (m)	R (Ωm^2)	S (Ω^{-1})	Layer lithological description	K (m/d)	T (m^2/d)	Σ S (Ω^{-1})
11	1	113	4.82	544.6	0.04	Superficial deposits	–	–	1.7
	2	21.5	27.3	586.9	1.27	Clay	–	–	
	3	85.1	32.4	2757.2	0.38	Sand (Aquifer)	6.11	198.3	
	4	176	–	–	–	Sandstone (aquifer)	3.1	–	
12	1	135	5.9	796.5	0.04	Superficial deposits	–	–	1.9
	2	23.5	32.9	773.2	1.4	Clay	–	–	
	3	96	40.4	3878.4	0.42	Sand (Aquifer)	5.46	220.9	
	4	199	–	–	–	Sandstone (aquifer)	2.77	–	
13	1	104	7.6	790.4	0.07	Superficial deposits	–	–	3
	2	21.1	48.3	1019.1	2.29	clay	–	–	
	3	91.3	21.4	1953.8	0.23	Sand (Aquifer)	5.73	122.6	
	4	36.5	15.2	554.8	0.41	Mudstone	–	–	
	5	195	–	–	–	Sandstone (aquifer)	2.82	–	

Profile 2 is formed from S 6, S 7, S 8 and S 9 and is composed of 4 geoelectric layers (Figs. 6b and 7b). The first layer of superficial deposits has an average thickness of 6 m, followed by a clay layer with a thickness that varies between 22.7 and 32.1 m and an average resistivity of 17 Ωm. The third layer is interpreted as saturated sand with an average thickness of 31 m and a resistivity range from 108 to 173 Ωm. This aquiferous layer is underlaid by aquitard composed of mudstone of an average thickness of 36 m. The fifth layer is interpreted as saturated sandstone with resistivity varying between 166 and 192 Ωm.

Profile 3 consists of S 10, S 11, S 12 and S 13. This profile comprises 5 geological units (Figs. 6c and 7c). Superficial deposits of an average thickness and resistivity of 6 m 120 Ωm represent the first layer. The second layer is interpreted as clay with an average thickness of 37 m, followed by saturated sand with thickness and resistivity ranging from 21.4 to 40.4 m and 85.1–96 Ωm, respectively. The aquiferous layer is underlaid by an aquitard composed of mudstone. This layer appeared only in VES 10 and VES 13, since reverse faulting drove the mudstone layer upwards and was later removed by erosion. The bottom layer in this profile is saturated sandstone of resistivity that varies between 176 and 199 Ωm.

It can be concluded from the integration of the electrical sounding and the lithological logs that two water-bearing formations are hosting groundwater in the study area. The upper aquifer comprises sand with thicknesses ranging from 20 to 100 m, and the lower aquifer is of relatively coarse sandstone with thicknesses up to 200 m. These two aquifers are hydraulically connected and separated by a reasonably thick aquitard composed of mudstone. The obtained results are compatible with the studies of

Dar Zarrouk and hydrogeological parameters

The aquifer characteristics are successfully described in this study using Dar Zarrouk parameters. The Dar Zarrouk characteristics lessen the uncertainty in interpreting geoelectrical data when identical lithologies overlap (Hasan et al. 2019). The calculated parameters are shown in Table 4. The groundwater aquifer in the studied area has a transverse resistance (R) that ranges from 141 to 13240.5 Ωm^2. In Fig. 8a, the areal distribution of R is illustrated. The presence of fine materials or a thin aquifer is more likely an indicator of the lowest value of R than low potentiality (Ezeh 2012). The S 4 station has the lowest value in this investigation, while the highest value is observed in the S 1 location. As shown in Fig. 8b, S 1 in the central region exhibits the highest longitudinal conductance (S) value (2.76 Ω^{-1}), whereas S 3 exhibits the lowest (0.008 Ω^{-1}). The greatest S value suggests good aquifer productivity, since it reflects a high groundwater flow rate (Kelly and Reiter 1984). The groundwater flow rate per unit cross-sectional area is represented by the hydraulic conductivity (K). Other petrophysical factors such as porosity, shale content, and water content significantly impact K. In this study, Heigold et al. (1979) empirical equation is used to determine hydraulic conductivity. The K ranges from 1.93 m/d in S 9 to 6.11 m/d in S 11. The spatial distribution of K for the upper aquifer is illustrated in Fig. 8c. As conducted VES measurement cannot show the thickness of the lower aquifer, the transmissivity (T) is only evaluated for the upper groundwater aquifer. The T values range from 114.2 to 413 m^2/d, and the spatial variation in the research area is depicted in Fig. 8d. The highest T is detected in S 5 in the middle region of the area, where a thick layer of coarse sandstone is observed, while S 7 showed the lowest T as a result of the low thickness of the aquifer.

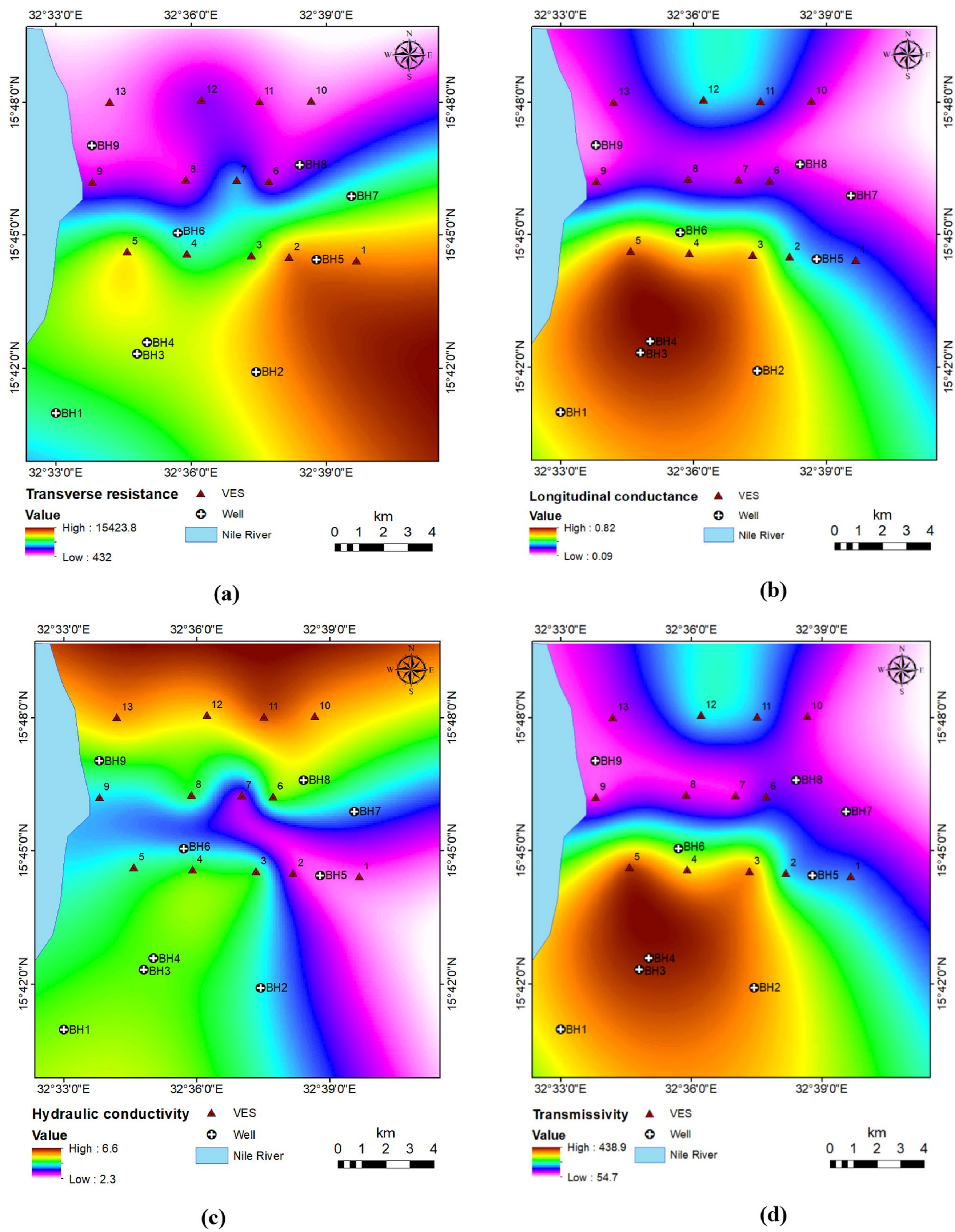

Fig. 8 Spatial distribution of **a** transverse resistance, **b** longitudinal conductance, **c** hydraulic conductivity, and **d** transmissivity for the upper aquifer

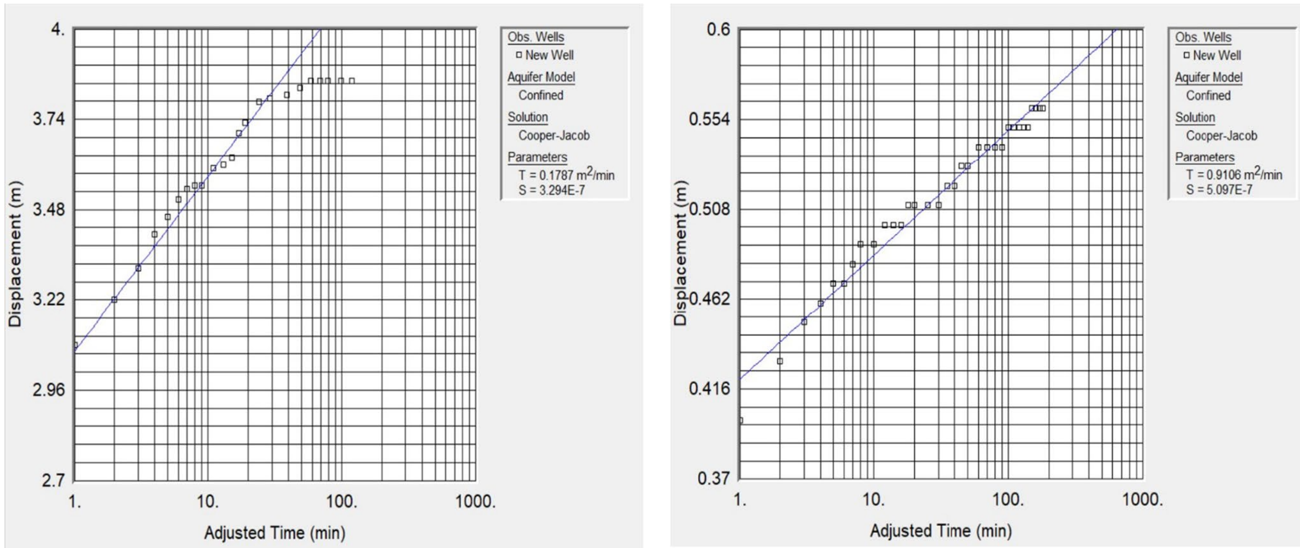

(a) (b)

Fig. 9 Result of pumping test analysis using Cooper–Jacob (1946) method for **a** BH 5 and **b** BH 1

The pumping data of BH 5 and BH 1 are analyzed to detect the hydrogeological parameters for the shallow and deep aquifers. The pumping tests were used to validate the results obtained from Dar Zarrouk parameters. For BH 5 (Fig. 9a), installed in the upper zone, the aquifer is pumped for 180 min with a pumping rate of 456 m^3/d until the steady state condition is reached. Consequently, a transmissivity of 257 m^2/d is calculated. This result shows a close agreement with the nearest VES station (VES 2), which indicated a hydraulic conductivity and transmissivity of 2.99 m/d and 215 m^2/d. Elkrail and Adlan (2019) and Algafar et al. (2011) predicted almost the same values. BH 1 is installed in the lower zone and pumped with 1200 m^3/d. The obtained transmissivity is up to 1300 m^2/d (Fig. 9b). The detection of transmissivity of the lower aquifer zone using the geophysical data is restricted, since the depth of penetration of the current survey is 200 m, while the thickness of the deep aquifer is up to 300 m (Farah et al. 1997). However, the obtained results are compatible and valuable in aquifer characterization. According to these results, it can be concluded that the Nubian aquifer in Khartoum state is moderately productive and ideal for groundwater development.

The relationships between the hydrogeological and Dar Zarrouk parameters are revealed using regression analysis. A high correlation between every two parameters suggests a strong relationship and high dependency between them. As illustrated in Fig. 10, S and R are moderately correlated with K with correlation coefficients (r) of 0.79 and 0.51, respectively. The groundwater flow rate is highly influenced by ρ and S; thus, K strongly correlates with ρ ($r=95$), and T is highly correlated with longitudinal conductance ($r=99$). In this study, the result of regression analysis led to the development of a local connection between Dar Zarrouk and hydrogeological parameters. Equation 13 through 16 can be used to calculate these parameters within the study area.

$$K = 8.14 + (-0.03\rho) \tag{13}$$

$$T = 0.56 + 531.3 * S \tag{14}$$

$$R = 19696.7 + (-2938.3K) \tag{15}$$

$$S = 0.2 + 0.04K \tag{16}$$

Longitudinal conductance determines the capacity of the geological layers to resist surface and subsurface contamination (Bayewu et al. 2018). The longitudinal conductance and the vertical and horizontal hydraulic conductivity are inversely related to the protective capability of the underlying materials. In this research, the vulnerability of the aquifer is evaluated based on Oladapo and Akintorinwa (2007) criteria. The protective capacity ranges from good to very good, since the aquifers in the research area are restricted to semi-confined. The protective capacity is limited, and the aquifer is vulnerable to pollution if the groundwater aquifer is shallow and the materials that cover it are thin and permeable. The protective strength of groundwater aquifers is depicted in Fig. 11. Where a thick clay layer is indicated, S 1 and S 2 having the maximum protective capacity with a very good class and due to the lack of an aquitard layer, S 11 station has the lowest protective capacity with a good class. In general, it can be indicated that the aquifers in eastern

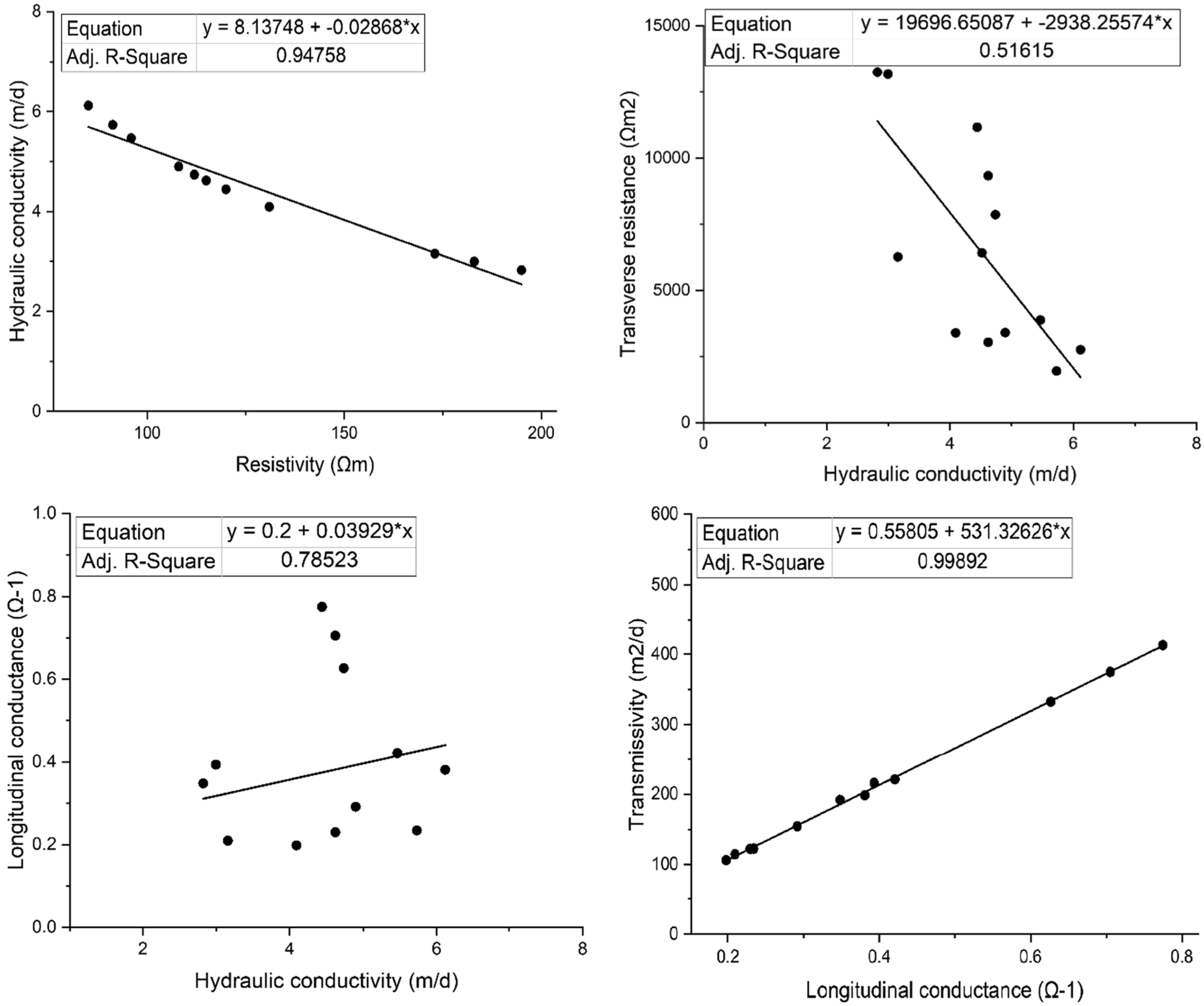

Fig. 10 Regression analysis between Dar Zarrouk parameters and hydrogeological parameters

Nile River area are highly protected from surface and subsurface contamination, and the groundwater is likely to be of good quality.

Hydrochemical analysis

General hydrochemistry

In this study, the detected physiochemical parameters are pH, TH, TDS, EC, Na^{+}, Ca^{+2}, Mg^{+2}, HCO_3^{-} Cl^{-} SO_4^{-2}, and NO_3^{-}. The result of the hydrochemical analysis is illustrated in Tables 5 and 6 shows the descriptive statistics of the analyzed parameters. The range of groundwater pH is from 7.2 to 7.9, and the acceptable pH values for groundwater are from 6 to 8.5 WHO (Edition 2011). According to pH values, groundwater is considered neutral to alkaline. TDS is one of the key metrics used to evaluate groundwater contamination levels. Classifying groundwater according to TDS is crucial to assess its suitability for all uses (Freeze and Cherry 1979). TDS ranged from 190.2 to 1050 mg/L. WHO (Edition 2011) advised that a TDS level of 600 mg/L is ideal for drinking. In this study, only one groundwater sample exceeded the prescribed limits. Fresh groundwater is defined as having a TDS concentration below 1000 mg/L, brackish groundwater as having a TDS concentration between 1000 and 10,000 mg/L, and saline groundwater as having a TDS value beyond 10,000 mg/L WHO (Edition 2011). In this research, 8 out of 9 groundwater samples were classified as freshwater, while one was defined as brackish water. EC varies between 317 and 1500 µS/cm, and the standard limit for the EC of groundwater is 750 µS/cm WHO (Edition 2011). TH of groundwater varies between 124 and 380 mg/L. In this

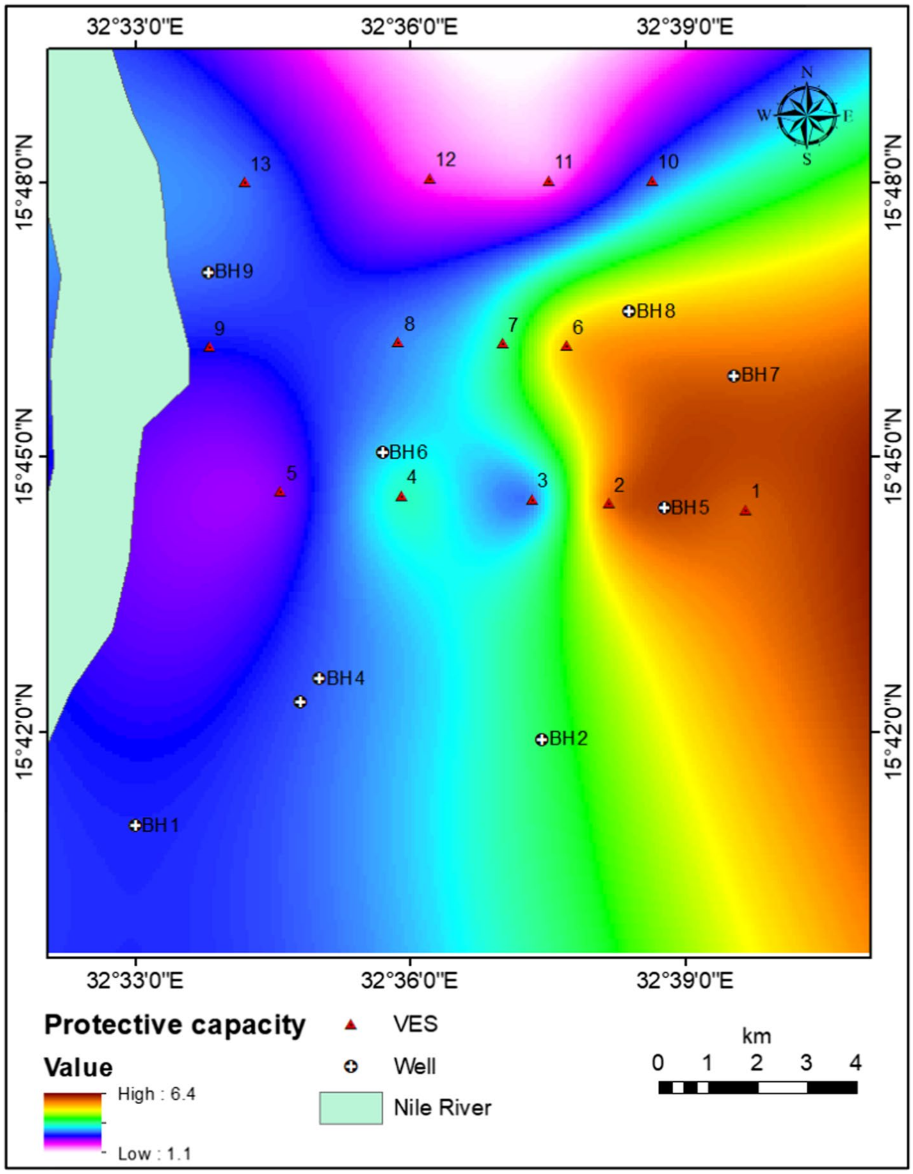

Fig. 11 Areal distribution of the protective capacity of the geological column in the study area

Table 5 Physiochemical parameters used in the calculation of GWQI

BH no.	pH	EC (mg/L)	TDS (mg/L)	TH (mg/L)	Cl^- (mg/L)	SO^{-2}_4 (mg/L)	NO^-_3 (mg/L)	Ca^{+2} (mg/L)	Mg^{+2} (mg/L)	Na^+ (mg/L)	HCO^-_3 (mg/L)	WQI
BH1	7.4	370	222	160	4	3	7.3	39.2	14.88	14.4	186	41.5
BH2	7.9	317	190.2	124	20	13	3.7	27.2	13.44	24.13	130	34.8
BH3	7.4	590	354	208	8	28	1.2	40.3	25.44	37.2	248	56.7
BH4	7.2	585	322	200	12	27.9	3	38.4	25	46.83	250	55.8
BH5	7.9	1500	1050	380	193	320.5	0.07	16	82.62	332.8	414.8	148
BH6	7.4	598	359	148	24	53	3.5	30.4	17.28	74.7	212	52.6
BH7	7.7	1318	724.9	300	120	100	2.8	44	45.6	147.52	340	104
BH8	7.7	929	694.4	260	91.5	152	7.5	57.6	28.2	123	292.8	94.1
BH9	7.4	518	362.6	185	23.9	23	6.2	38.4	22.356	45.89	281.6	55.6

Table 6 Descriptive statistics for the analyzed parameters

Parameter	Minimum	Mean	Maximum	WHO (Edition 2011) standard
pH	7.2	7.6	7.9	6.5–8.5
EC	317	747	1500	750
TDS	190.2	475	1050	600
TH	124	218	380	100
Cl^-	4	55	193	250
SO^{-2}_4	3	80	320.5	200
NO^-_3	0.07	3.9	7.5	45
Ca^{+2}	16	36.8	57.6	75
Mg^{+2}	13.4	30.5	82.6	150
Na^+	14.4	94	332.8	200
HCO^-_3	130	261.7	414.8	350
GWQI	34.8	91.4	148	–

analysis, eight groundwater samples are classified as hard, whereas one sample is considered very hard water. In hydrochemistry, Na^+ is the dominant cation used to identify the suitability of groundwater for drinking and agricultural purposes. BH 5 showed the highest concentration (332.8 mg/L), whereas BH 1 had the lowest (14.4 mg/L). Ca^{+2} concentration ranged between 16 and 57.6 mg/L, and the maximum concentration was recorded in BH 8. The content of Mg + 2 ranged from 13.4 to 82.6 mg/L. Ca^{+2} and Mg^{+2} are the key parameters used to detect groundwater hardness. HCO_3^- is the predominant anion in the research area, and its concentration ranges from 130 to 414.8 mg/L. The range of SO_4^{-2} concentrations is from 3 to 320.5 mg/L. Cl^- concentration ranges from 4 to 193 mg/L. The lowest concentration was found in BH 1, and the highest concentration was found in BH 5. The range of NO_3^- concentration is 0.07 to 7.5 mg/L and BH 8 records the highest concentration, while BH 5 records the lowest concentration. Agriculture is the primary source of NO_3^- in the environment (Mohammed et al. 2023a). The geographical distribution of the physiochemical parameters is shown in Fig. 12. The areal dispersion of Na^+, Mg^{+2}, Cl^-, SO_4^{-2}, TH, and TDS follow a similar pattern as their concentrations grow from the western to the eastern part of the study area. This may indicate that these parameters are of the same origin and water–rock interaction is likely to be the source of these parameters.

Hydrochemical facies

The evaluation of hydrogeochemical facies aids in identifying the groundwater flow characteristics and chemical evolution as different geochemical mechanisms impact groundwater chemistry (Chung et al. 2015). In this study, Piper (1944) diagram is projected to evaluate the geochemistry of the groundwater samples and, thus, reveal the hydrochemical facies. Figure 13 illustrates the Piper plot in which groundwater samples are plotted in the cations and anions triangles and then projected into the central diamond shape. In the anions triangle the plot indicated that most of the samples are dominated with HCO^-_3, while the cations almost equally contributed to overall chemistry. In multidimensional central diamond, most groundwater samples, including BH 1, BH 2, BH 3, BH 4, and BH 9, are dominated by Ca–Mg–HCO_3 hydrochemical facies. These boreholes are located in the western part within the radius of the Nile River influence and are directly recharged from the Nile River. Therefore, the chemical composition of these samples is influenced by the composition of the Nile River water, which is rich in Ca^{+2} and HCO^-_3 (Mohammed et al. 2022c). The spatial distribution of these ions also confirms this, as it behaves differently from the remaining parameters. Mineral dissolution, especially calcite and dolomite, can also cause this groundwater type. Three samples, including BH 6, BH 7 and BH 8, are projected in the mixed water zone. The mixed facies is a result of mixing different types of water. Sample of BH 5 which is located in eastern part of the area is plotted in Na–Cl hydrochemical facies. This water type is likely to be produced by the cation exchange reaction in which Ca^{+2} and Mg^{+2} are replaced by Na^+ along the flow path (Yadav et al. 2018). It can be concluded that rock-water interactions and the cation exchange process are the main factors influencing groundwater chemistry in the eastern Nile River.

Groundwater quality index (GWQI)

To assess the quality of the groundwater in the vicinity of the eastern Nile River, GWQI is calculated. Since there are no measures of microbiological contamination in the research region, the definition of the groundwater quality index is limited in this study. However, the routinely measured physiochemical parameters can efficiently evaluate the suitability of the groundwater for drinking purposes. The computed GWQI varies between 34.8 and 148; eventually, groundwater samples were classified into three groups. Two samples of BH 1 and BH 2 fall into the excellent groundwater category, while BH 3, BH 4, BH 6, BH 8, and BH 9 represent the good category and samples of BH 5 and BH 7 fall into a poor water type. Figure 14 illustrates the spatial variation of GWQI. The minimum GWQI is recorded in BH 2 in the south part of the area, while the maximum is in BH 5 in the eastern part of the study area. The high GWQI at BH 5 is influenced by the high concentration of TDS, SO^{-2}_4, Na^+, and HCO^-_3, since the concentrations of these parameters are above the standard limit prescribed by WHO (Edition 2011). Based on the calculated GWQI, the groundwater in the study area is suitable for drinking except for BH 5 and BH 7. However, specific physiochemical characteristics influence some groundwater samples. Since advection and dispersion mechanisms may distribute contamination

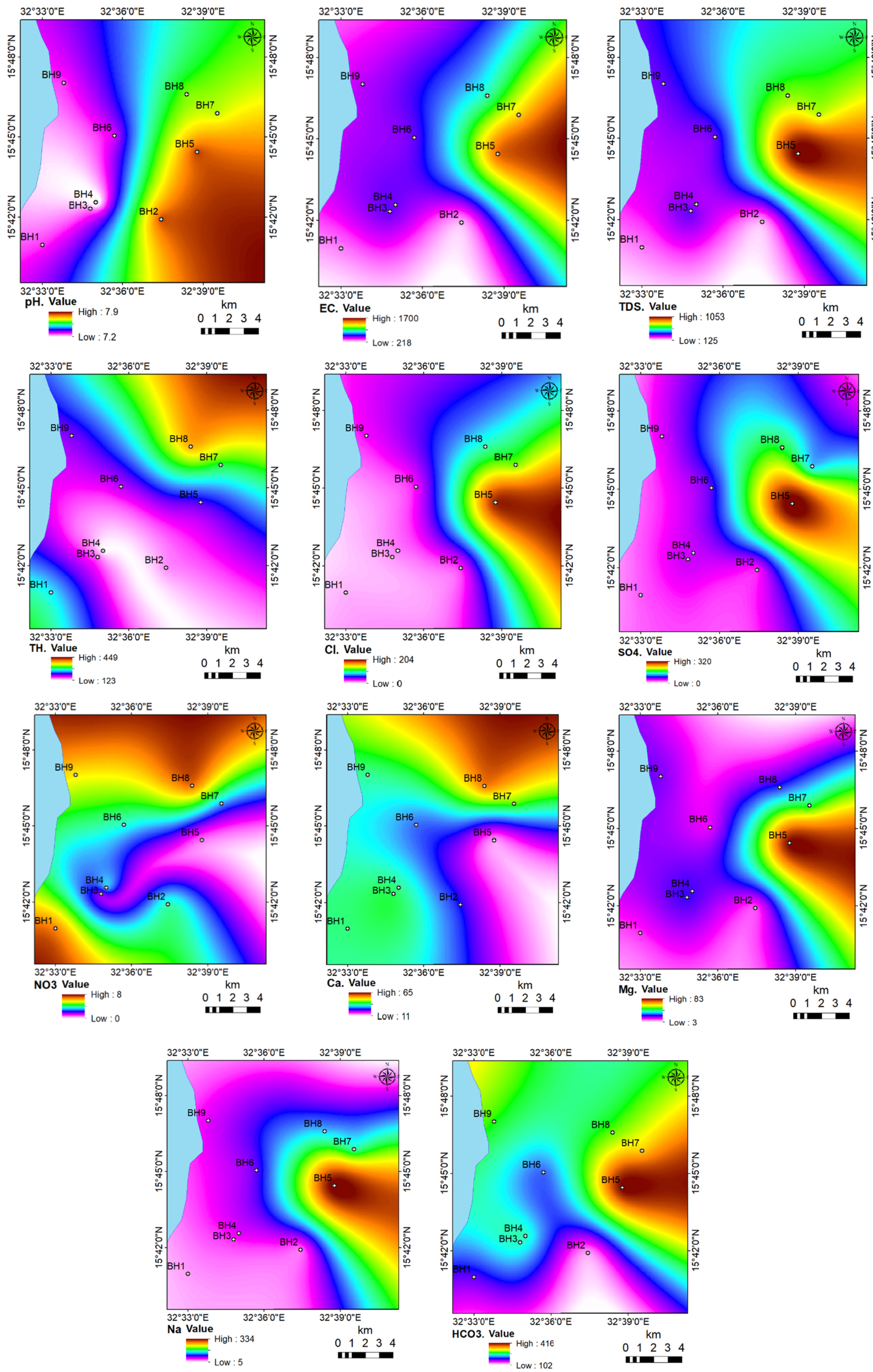

Fig. 12 Areal distribution of the physiochemical parameters used in the calculation of GWQI

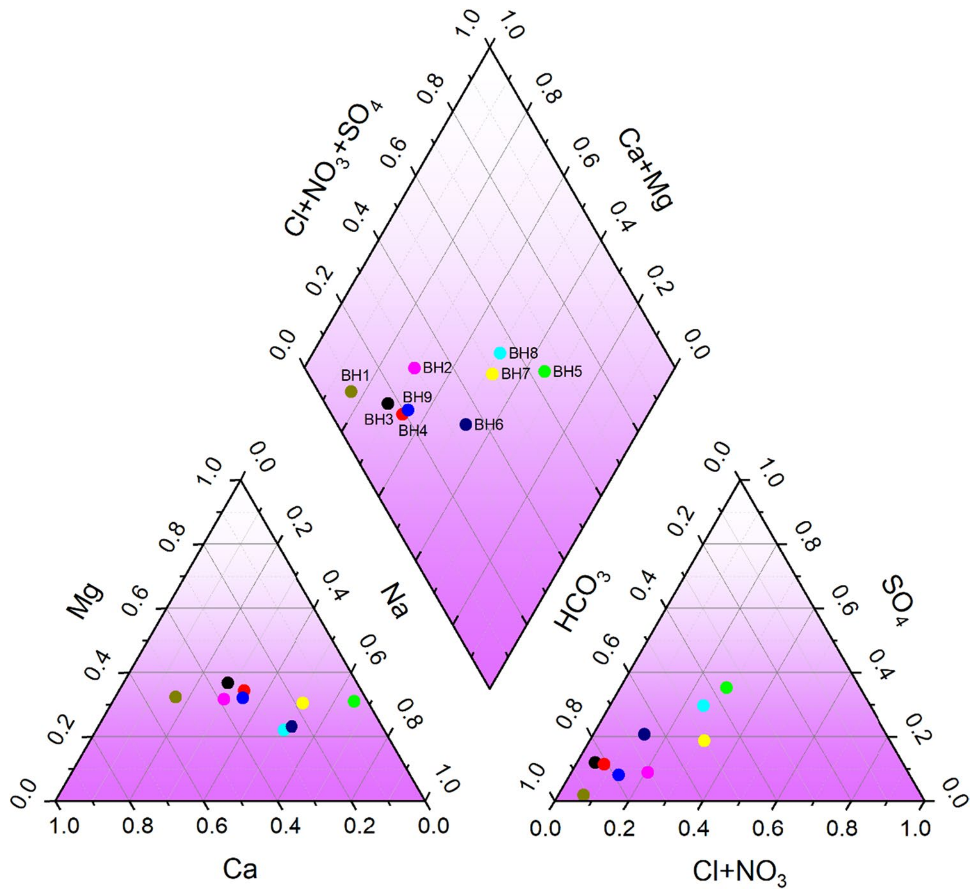

Fig. 13 Piper diagram shows the main hydrogeological facies in the study area

throughout the groundwater flow routes (Mohammed et al. 2022b), this may significantly impact the current groundwater quality situation. Therefore, competent authorities should create suitable plans for maintaining and improving the current state of the drinking water supply in the eastern Nile River region.

Conclusions

This research aims to comprehensively characterize groundwater aquifer in the eastern Nile River area, Khartoum state, following an integrated approach using geophysical and hydrochemical methods. A geoelectrical resistivity survey using vertical electrical sounding (VES) technique was employed to delineate and explore groundwater potentialities in the study area. VES data were interpreted using the 1D least damped square geophysical inversion technique guided by lithological logs obtained from 8 drilled boreholes. The results showed that the study area comprises two hydraulically connected aquifer systems. An upper aquifer of sand with an average thickness of 50 m and a lower aquifer composed of coarse sandstone with thicknesses up to 200 m. Dar Zarrouk parameters, namely, transverse resistance and longitudinal conductance, are measured using VES inversion results with average values of 6690 Ωm^2 and 1.4 Ω^{-1}, respectively. Consequently, the hydrogeological parameters, including hydraulic conductivity and transmissivity, are measured to detect the productivity of the groundwater aquifers. Regression analysis between Dar Zarrouk and hydraulic parameters is performed to develop a local relationship for estimating aquifer parameters within the study area. Longitudinal conductance was further used to predict the protective capacity of the groundwater aquifers. It was indicated that the overall protective strength of the hydrogeological columns is good, which suggests good water quality. This result was further confirmed with the groundwater quality index model. Weighted arithmetic GWQI was employed to assess groundwater quality in the study area using physiochemical parameters obtained from 9 boreholes. Consequently, groundwater was classified into three groups: excellent, good, and poor groundwater. It can be concluded from the obtained results that groundwater in the study area is in an ideal situation for groundwater exploitation. However, for a comprehensive evaluation and management of groundwater resources in the eastern River Nile area, we recommend.

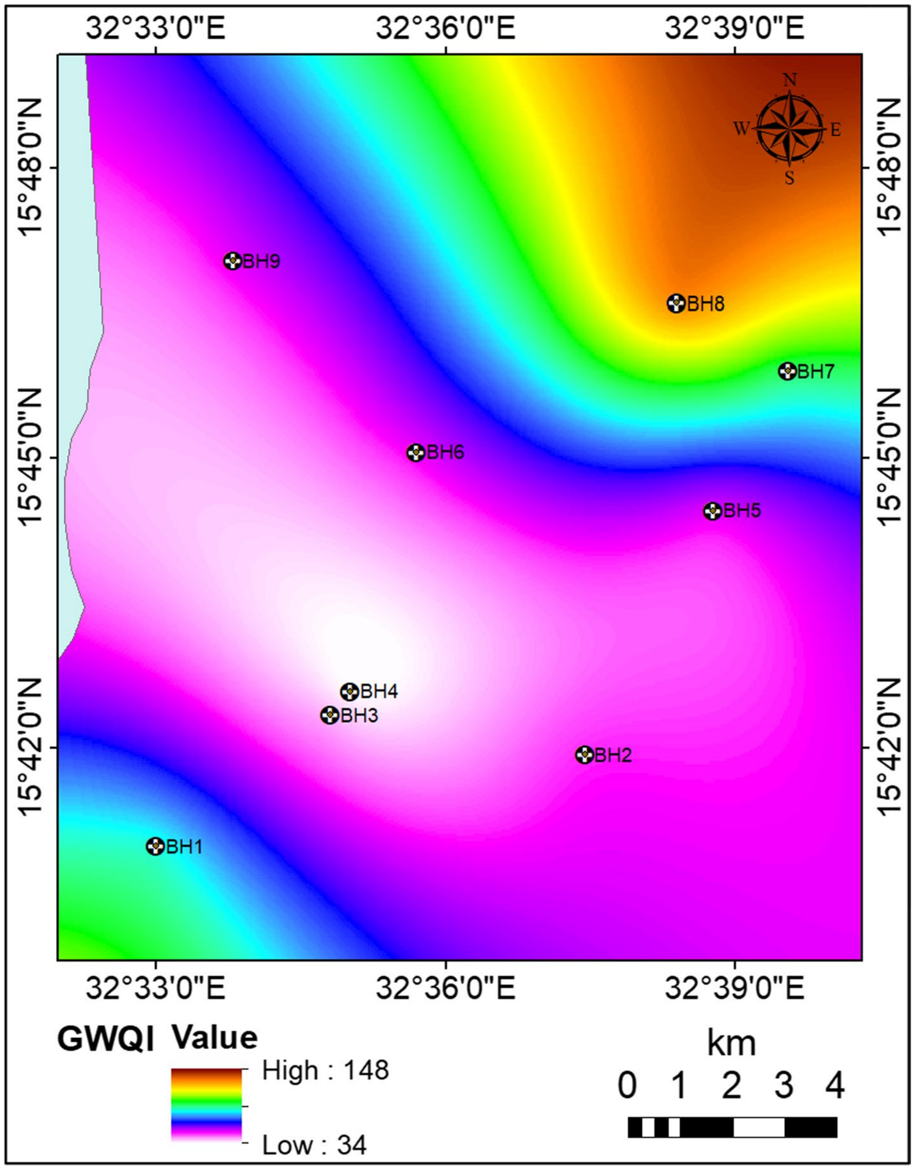

Fig. 14 Spatial variation of GWQI in the study area

- Applying a detailed geophysical survey to reduce the uncertainty of the resulting geological and hydrogeological models. For instance, geophysical well-logging methods can calibrate VES measurement in delineating water-saturated zones and detecting the petrophysical parameters, such as porosity, permeability, and hydraulic conductivity.
- Conducting electrical resistivity tomography (ERT) with 2D geophysical inversion to detect and estimate the aquifer geometry and hydrogeological parameters accurately. Time-lapsed ERT measurement can successfully provide information on groundwater pollutant sources and spread patterns.
- Installation of groundwater quality monitoring scheme for proper management of groundwater resources to ensure water supply sustainability.

Author contributions MAAM: methodology, data analysis, figures preparation, original draft writing. NPS: interpretation of VES data, editing and supervision. PS: development of GWQI model, editing and supervision.

Funding Open access funding provided by University of Miskolc. The authors declare that no funds are received during this work.

Data availability Not applicable.

Declarations

Conflict of interest The authors declare no competing interests.

Ethical approval The authors confirm that all the research meets ethical guidelines.

Consent to participate Not applicable.

Consent to publish The authors declare that this work does not contain any material from any individual.

References

Abdelsalam YE, EA EM, Elhadi H El (2016) Problems and factors which retard the development and the utilization of groundwater for drinking purposes in the Khartoum state-SUDAN. In: 7th International Conference on Environment and Engineering Geophysics \& Summit Forum of Chinese Academy of Engineering on Engineering Science and Technology. Dordrecht, pp 449–451

Akhter G, Hasan M (2016) Determination of aquifer parameters using geoelectrical sounding and pumping test data in Khanewal District, Pakistan. Open Geosci 8:630–638. https://doi.org/10.1515/geo-2016-0071

Algafar MA, Abdou G, Abdelsalam Y (2011) Groundwater flow model for the Nubian aquifer in the Khartoum area, Sudan. Bull Eng Geol Environ 70:619–623. https://doi.org/10.1007/s10064-011-0366-7

Appelo CAJ, Postma D (2005) Geochemistry, groundwater and pollution, 2nd edn. Balkema, Rotterdam

Araffa SAS, Abdelazeem M, Sabet HS, Dabour AMA (2021) Hydrogeophysical investigation at El Moghra Area, North Western Desert, Egypt. Environ Earth Sci 80:1–17. https://doi.org/10.1007/s12665-020-09332-5

Asadi E, Isazadeh M, Samadianfard S et al (2020) Groundwater quality assessment for sustainable drinking and irrigation. Sustainability 12:177

Attwa M, Basokur AT, Akca I (2014) Estimation de la conductivité hydraulique à partir de données de sondages avec courant direct: Un cas d'étude dans l'Est du Delta du Nil, Egypte. Hydrogeol J 22:1163–1178. https://doi.org/10.1007/s10040-014-1107-3

Bayewu OO, Oloruntola MO, Mosuro GO et al (2018) Assessment of groundwater prospect and aquifer protective capacity using resistivity method in Olabisi Onabanjo University campus, Ago-Iwoye, Southwestern Nigeria. NRIAG J Astron Geophys 7:347–360. https://doi.org/10.1016/j.nrjag.2018.05.002

Boateng TK, Opoku F, Acquaah SO, Akoto O (2016) Groundwater quality assessment using statistical approach and water quality index in Ejisu-Juaben Municipality, Ghana. Environ Earth Sci 75:1–14. https://doi.org/10.1007/s12665-015-5105-0

Brown RM, McClelland NI, Deininger RA, Tozer RG (1970) A water quality index-do we dare. Water Sewage Works 117:339–343

Chung SY, Venkatramanan S, Kim TH et al (2015) Influence of hydrogeochemical processes and assessment of suitability for groundwater uses in Busan City, Korea. Environ Dev Sustain 17:423–441

Cooper HH Jr, Jacob CE (1946) A generalized graphical method for evaluating formation constants and summarizing well-field history. EOS Trans Am Geophys Union 27:526–534

Daud S, MonaLisa, Nisar UB (2022) Integrated geophysical, geochemical, and geospatial tools to characterize water resources in GAIE, Eastern Peshawar basin, Pakistan. Environ Earth Sci 81:1–19. https://doi.org/10.1007/s12665-022-10516-4

de Almeida A, Maciel DF, Sousa KF et al (2021) Vertical electrical sounding (Ves) for estimation of hydraulic parameters in the porous aquifer. Water (switzerland). https://doi.org/10.3390/w13020170

Edition F (2011) Guidelines for drinking-water quality. WHO Chron 38:104–108

Elkrail AB, Adlan M (2019) Groundwater flow assessment based on numerical simulation at omdurman area, Khartoum State, Sudan. Afr J Geosci 2:59–65

Eyankware MO, Akakuru OC, Eyankware OE (2022) Hydrogeophysical delineation of aquifer vulnerability in parts of Nkalagu area of Abakaliki, se. Nigeria. Sustain Water Resour Manag 8:1–19. https://doi.org/10.1007/s40899-022-00603-6

Ezeh CC (2012) Hydrogeophysical studies for the delineation of potential groundwater zones in Enugu state, Nigeria. Int Res J Geol Min 2:103–112

Farah EA, Abdullatif OM, Kheir OM, Barazi N (1997) Groundwater resources in a semi-arid area: a case study from central Sudan. J Afr Earth Sc 25:453–466

Farah EA, Mustafa EMA, Kumai H (2000) Sources of groundwater recharge at the confluence of the Niles, Sudan. Environ Geol 39:667–672

Freeze RA, Cherry JA (1979) Groundwater. Prentice-hall

Gugulothu S, Dhakate R, Sreedhar K et al (2020) Geophysical and hydrochemical studies for sustainable development of groundwater resources in northwestern part of Telangana State, India. J Earth Syst Sci. https://doi.org/10.1007/s12040-020-01452-7

Haggaz YAS, Kheirallah KM (1988) Paleohydrology of the Nubian aquifer northeast of the Blue Nile, near Khartoum, Sudan. J Hydrol 99:117–125

Hasan M, Shang Y, Akhter G, Jin W (2019) Application of VES and ERT for delineation of fresh-saline interface in alluvial aquifers of Lower Bari Doab, Pakistan. J Appl Geophys 164:200–213

Heigold PC, Gilkeson RH, Cartwright K, Reed PC (1979) Aquifer transmissivity from surficial electrical methods. Groundwater 17:338–345

Hussein MT, Awad HS (2006) Delineation of groundwater zones using lithology and electric tomography in the Khartoum basin, central Sudan. CR Geosci 338:1213–1218. https://doi.org/10.1016/j.crte.2006.09.007

Ige OO, Adunbarin OO, Olaleye IM (2022) Groundwater potential and aquifer characterization within Unilorin campus, Ilorin, Southwestern Nigeria, using integrated electrical parameters. Int J Energy Water Resour. https://doi.org/10.1007/s42108-021-00160-2

Kanga IS, Naimi M, Chikhaoui M (2020) Groundwater quality assessment using water quality index and geographic information system based in Sebou River Basin in the North-West region of Morocco. Int J Energy Water Resour 4:347–355

Kelly WE, Reiter PF (1984) Influence of anisotropy on relations between electrical and hydraulic properties of aquifers. J Hydrol 74:311–321

Kheiralla MK (1966) Study of the Nubian Sand stone Formation of the Nile Vally between 14 N and 17 42 N, with reference to groundwater geology. University of Khartoum

Köhnke M, Skala W, Erpenstein K (2017) Nile groundwater interaction modeling in the northern Gezira plain for drought risk assessment. Geoscientific research in Northeast Africa. CRC Press, pp 705–711

Mahmud S, Hamza S, Irfan M et al (2022) Investigation of groundwater resources using electrical resistivity sounding and Dar Zarrouk parameters for Uthal Balochistan, Pakistan. Groundw Sustain Dev 17:100738–100739. https://doi.org/10.1016/j.gsd.2022.100738

Maillet R (1947) The fundamental equations of electrical prospecting. Geophysics 12:529–556

Mohammed MAA (2020) The use of Landsat ETM+ in hydrogeological investigation in basement terrain, Hamissana area, N-E Sudan. Hum Nat Sci J 1:370–378. https://doi.org/10.53796/hnsj1625

Mohammed MAA, Khleel NAA, Szabó NP, Szűcs P (2022a) Modeling of groundwater quality index by using artificial intelligence algorithms in northern Khartoum State, Sudan. Model Earth Syst Environ. https://doi.org/10.1007/s40808-022-01638-6

Mohammed MAA, Khleel NAA, Szabó NP, Szűcs P (2022b) Development of Artificial intelligence model with aid of statistical methods for simulation of water quality indices in north Khartoum area, Sudan. Res Square. https://doi.org/10.21203/rs.3.rs-1679487/v1

Mohammed MAA, Szabó NP, Szűcs P (2022c) Multivariate statistical and hydrochemical approaches for evaluation of groundwater quality in north Bahri city-Sudan. Heliyon 8:e11308. https://doi.org/10.1016/J.HELIYON.2022.E11308

Mohammed MAA, Eltijani A, Szabó NP, Szűcs P (2023a) Multi-criterion approach for assessment of hydrochemical characteristics and human health risk of groundwater in Khartoum State, Sudan. Res Square. https://doi.org/10.21203/rs.3.rs-2481210/v1

Mohammed MAA, Szabó NP, Szűcs P (2023b) Exploring hydrogeological parameters by integration of geophysical and hydrogeological methods in northern Khartoum state, Sudan. Groundw Sustain Dev 20:100891. https://doi.org/10.1016/j.gsd.2022.100891

Muhammad S, Ehsan MI, Khalid P (2022) Optimizing exploration of quality groundwater through geophysical investigations in district Pakpattan, Punjab, Pakistan. Arab J Geosci. https://doi.org/10.1007/s12517-022-09990-8

Niwas S, Singhal DC (1981) Estimation of aquifer transmissivity from Dar-Zarrouk parameters in porous media. J Hydrol 50:393–399. https://doi.org/10.1016/0022-1694(81)90082-2

Nugraha GU, Nur AA, Pranantya PA et al (2022) Analysis of groundwater potential zones using Dar-Zarrouk parameters in Pangkalpinang city, Indonesia. Environ Dev Sustain. https://doi.org/10.1007/s10668-021-02103-7

Oladapo MI, Akintorinwa OJ (2007) Hydrogeophysical study of ogbese south western Nigeria. Global J Pure Appl Sci 13:55–61

Oyeyemi KD, Aizebeokhai AP, Metwaly M et al (2021) Evaluating the groundwater potential of coastal aquifer using geoelectrical resistivity survey and porosity estimation: a case in Ota, SW Nigeria. Groundw Sustain Dev 12:100488. https://doi.org/10.1016/j.gsd.2020.100488

Piper AM (1944) A graphic procedure in the geochemical interpretation of water-analyses. EOS Trans Am Geophys Union 25:914–928

Ramakrishniah CR, Sadashivaiah C, Ranganna G (2009) Assessment of water quality index for the groundwater in Tumkur Taluk. E-J Chem 6:523–530

Sharifinia M, Adeli B, Nafarzadegan AR (2017) Evaluation of water quality trends in the Maroon River Basin, Iran, from 1990 to 2010 by WQI and multivariate analyses. Environ Earth Sci 76:781. https://doi.org/10.1007/s12665-017-7132-5

Singh DF (1992) Studies on the water quality index of some major rivers of Pune, Maharashtra. In: Proc Acad Environ Biol. pp 61–66

Stanly R, Yasala S, Oliver DH et al (2021) Hydrochemical appraisal of groundwater quality for drinking and irrigation: a case study in parts of southwest coast of Tamil Nadu, India. Appl Water Sci 11:1–20. https://doi.org/10.1007/s13201-021-01381-w

Szabó NP (2015) Hydraulic conductivity explored by factor analysis of borehole geophysical data. Hydrogeol J 23:869–882

Tiwari TN, Mishra MA (1985) A preliminary assignment of water quality index of major Indian rivers. Indian J Environ Prot 5:276–279

Yadav KK, Gupta N, Kumar V et al (2018) GIS-based evaluation of groundwater geochemistry and statistical determination of the fate of contaminants in shallow aquifers from different functional areas of Agra city, India: levels and spatial distributions. RSC Adv 8:15876–15889

Zhang Y, Jia R, Wu J et al (2022) Uncertain in WQI-based groundwater quality assessment methods: a case study in east of Beijing, China. Environ Earth Sci 81:202. https://doi.org/10.1007/s12665-022-10311-1